

Computer-Assisted Proofs in Dynamical Systems: A Case Study of a Heteroclinic Orbit in the Shimizu–Morioka System

Olivier Hénot ^{*} Akitoshi Takayasu [†]

Abstract

The radii polynomial approach is an a posteriori validation method based on the contraction of a quasi-Newton operator. We apply this strategy to give a computer-assisted proof of a transverse heteroclinic orbit in the Shimizu–Morioka system, validating the equilibria and eigenpairs, the local invariant manifolds via the parameterization method, and the connecting orbit via a boundary-value problem. For each subproblem we present a four-step procedure: (i) zero-finding formulation, (ii) approximate zero, (iii) approximate inverse, and (iv) bound estimates. This highlights the unifying structure behind the a posteriori validation method. Alongside the analysis, we include code snippets implemented in Julia [3] using the `RadiiPolynomial` [13] library.

1 Introduction

The Shimizu–Morioka system [30]

$$\dot{x} = y, \quad \dot{y} = x - ay - xz, \quad \dot{z} = -bz + x^2, \quad (1)$$

where a, b are real parameters, illustrates how complex dynamics can arise even in simple models. As with the Lorenz system [18], system (1) exhibits a *butterfly* shaped strange attractor, where trajectories visit the two *wings* A and B in any prescribed symbolic sequence. The invariant manifolds, attached to equilibria or periodic orbits, are central to the global picture of the dynamics. These objects, however, are notoriously difficult to obtain analytically, and in general come with limited (if any) quantitative information. This makes the study of invariant manifolds and their intersection a particularly compelling instance of a fundamental problem in dynamical systems that benefits from the assistance of the computer.

In this paper, we use the existence proof of a transverse heteroclinic orbit connecting two saddle equilibria of the Shimizu–Morioka system (see Figure 1) to guide the reader through the key ideas and techniques of a posteriori validation based on the radii polynomial approach. While the underlying theory is well established (see, e.g., [17]), our exposition pursues a more structural aim. We highlight that each subproblem of the proof (the validation of equilibria and eigenpairs, of local invariant manifolds, and of the connecting orbit) fits into the same four-step procedure, thereby revealing the common structure of the computer-assisted proof framework in both finite- and infinite-dimensional settings, and isolating what is problem specific from what belongs to the framework. In parallel, we provide code snippets accompanying the mathematical analysis to illustrate explicitly how it translates into concrete practical implementations. As much as possible, we keep the discussion elementary so that the article remains approachable for

^{*}National Taiwan University, Department of Mathematics, No. 1 Sec. 4 Roosevelt Rd., 10617 Taipei, Taiwan. olivierhenot@ntu.edu.tw.

[†]University of Tsukuba, Institute of Systems and Information Engineering, 1-1-1 Tennodai, Tsukuba, Ibaraki 305-8573, Japan. takitoshi@risk.tsukuba.ac.jp.

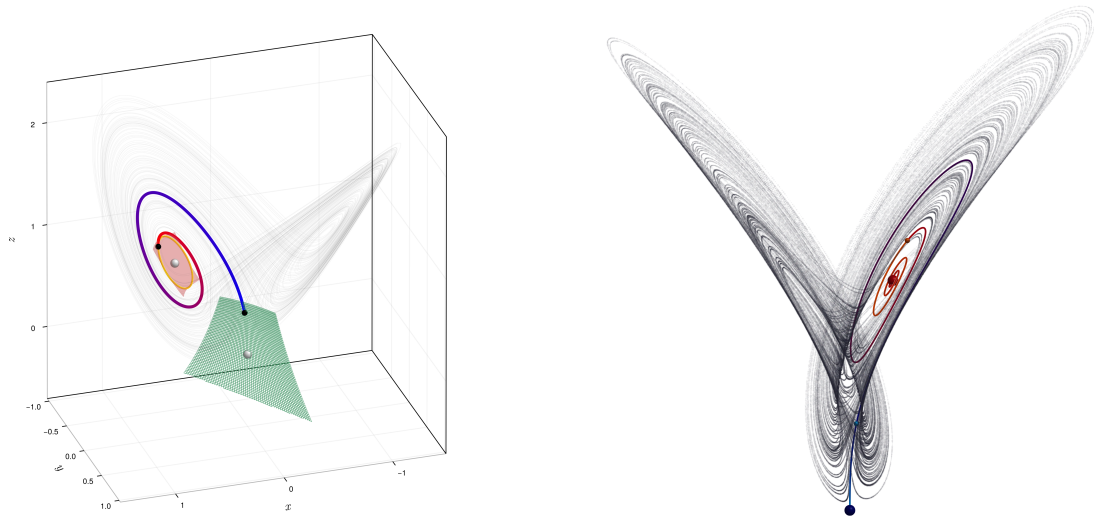


Figure 1: Transverse heteroclinic orbit connecting two saddle equilibria of the Shimizu–Morioka system, inside the strange attractor (shown in light grey).

newcomers; more experienced readers will find opportunities to improve the code (performance, memory management) and to sharpen the analytical bounds.

The difficulty of describing solutions to nonlinear differential equations has long motivated the development of practical theorems and algorithms to obtain approximate solutions. The fact that these efforts predate the digital computer by centuries [11] highlights the enduring need for reliable computational methods. The influence of the Japanese school of applied mathematics on the development of computer-assisted proofs must be acknowledged. Having embraced these methods early on, the Japanese school pioneered the field in many ways [31, 35, 19, 39], and continues to play a leading role today [22, 23, 25, 24, 27, 28, 20, 21]. The research and applications of computer-assisted proofs are rapidly growing [34, 15, 37, 16, 38, 12, 29, 32, 7, 10].

The article is organized as follows. Section 1.1 states the a posteriori validation framework used throughout the paper. Section 2 validates equilibria of the Shimizu–Morioka system and their stable and unstable eigenpairs. Section 3 validates Taylor series expansions of local parameterizations of the invariant manifolds via the parameterization method. Section 4 validates a Chebyshev series expansion of a segment of the transverse heteroclinic orbit connecting the two equilibria. The final section concludes with comments on the scope of the approach and possible extensions.

Software resources. The code accompanying this article, available at [14], is written in Julia [3], using the `RadiiPolynomial` [13] and `IntervalArithmetic` [2] software libraries. We also made use of the suite of ODE solvers from `DifferentialEquations` [26]. The figure in this article was made with `Makie` [9].

1.1 The radii polynomial approach

Many problems in dynamical systems are naturally formulated in the form of $F(x) = 0$. We begin this article by presenting a strategy to prove the existence of an isolated zero of F .

Let

- (i) \bar{x} be a numerical approximation of the zero (i.e., $F(\bar{x}) \approx 0$ numerically), and

(ii) A a numerical approximation of the inverse of $DF(\bar{x})$ (i.e., $A \approx DF(\bar{x})^{-1}$ numerically).

The following theorem gives sufficient conditions to prove the contraction of the quasi-Newton operator $x \mapsto x - AF(x)$ in an *explicit closed ball* of \bar{x} . We denote by $\mathcal{B}(X)$ the space of bounded linear operators from X to itself, while $B(\bar{x}, r)$ denotes the closed ball in X centered at \bar{x} with radius r . By convention, if $r = \infty$, then $B(\bar{x}, r) = X$.

Theorem 1.1 (Radii Polynomial Theorem). *Let X be a Banach space, $\bar{x} \in X$, $F : X \rightarrow X$ a C^1 map, and $A : X \rightarrow X$ an injective linear map. Fix $R \in [0, \infty]$, and let $Y, Z = Z(R) \geq 0$ be two positive constants satisfying*

$$\|AF(\bar{x})\|_X \leq Y, \quad \sup_{x \in B(\bar{x}, R)} \|I - ADF(x)\|_{\mathcal{B}(X)} \leq Z. \quad (2)$$

If $Z < 1$, then, for any $r \geq 0$ such that

$$\frac{Y}{1 - Z} \leq r \leq R, \quad (3)$$

the fixed-point operator $x \mapsto x - AF(x)$ is a contraction on $B(\bar{x}, r)$, so that there exists a unique zero $x^* \in B(\bar{x}, r)$ of F .

Proof. For $x \in B(\bar{x}, r)$, we have by the mean value inequality

$$\begin{aligned} \|x - AF(x) - \bar{x}\|_X &\leq \|AF(\bar{x})\|_X + r \int_0^1 \|I - ADF(\bar{x} + s(x - \bar{x}))\|_{\mathcal{B}(X)} \, ds \\ &\leq Y + rZ \\ &\leq r, \end{aligned}$$

which proves that $x \mapsto x - AF(x)$ is a map from $B(\bar{x}, r)$ to itself. Moreover, for $x, y \in B(\bar{x}, r)$,

$$\begin{aligned} \|x - AF(x) - (y - AF(y))\|_X &\leq \left(\sup_{\xi \in B(\bar{x}, r)} \|I - ADF(\xi)\|_{\mathcal{B}(X)} \right) \|x - y\|_X \\ &\leq Z \|x - y\|_X, \end{aligned}$$

which proves that $x \mapsto x - AF(x)$ is a contraction on $B(\bar{x}, r)$ since $Z < 1$. □

We interpret

1. Y as measuring the quality of the approximate zero \bar{x} of F .
2. $Z = Z(R)$ as measuring the quality of the approximate inverse A at \bar{x} , as well as quantifying the variation of the fixed-point operator $x \mapsto x - AF(x)$ over $B(\bar{x}, R)$.
3. R as an a priori error threshold, determining the ball for the $Z(R)$ bound. In special cases, one can take $R = \infty$, for instance when F is affine (so that DF is constant).

For a finite-dimensional space X , the Radii Polynomial Theorem 1.1 can be applied directly using interval arithmetic, as detailed in Section 2.1. Importantly, the injectivity of A need not be established a priori. Indeed, the condition $Z < 1$ implies that A is surjective, and, since X is finite-dimensional, A is a square matrix that must also be injective.

In contrast, when X is an infinite-dimensional function space, the procedure is less evident and requires analytical estimates to derive computable formulas for Y and Z . In this paper, we address the following questions: *How can analytic functions be modeled in a sequence space? How can nonlinearities be controlled in this setting? How can the estimates for the bounds Y and Z be reduced to a finite set of computations that can be carried out by the computer?*

2 Validated computation of equilibria and eigenspaces

The vector field of system (1) is given by

$$f(x, y, z) \stackrel{\text{def}}{=} \begin{pmatrix} y \\ x - ay - xz \\ -bz + x^2 \end{pmatrix}, \quad \text{and we choose the parameter values } a = \frac{3}{4}, b = \frac{9}{20}. \quad (4)$$

The implementation of the vector field f and its Jacobian Df is as follows.

<pre>function f(u, params) a, b = params x, y, z = u return [y x - a*y - x*z -b*z + x^exact(2)] end</pre>	<pre>function Df(u, params) a, b = params x, y, z = u return [zero(x) one(y) zero(z) exact(1)-z -a*one(y) -x exact(2)*x zero(y) -b*one(z)] end</pre>
---	---

Remark 2.1. *The functions f and Df above are written in a generic form so that they can be reused throughout the paper. In particular, two implementation choices deserve comment:*

1. *Integer literals are wrapped with `exact`. The `exact` function, provided by `IntervalArithmetic` [2], declares that the underlying number is to be treated as mathematically exact; arithmetic mixing an interval with such a number then retains rigorous semantics. Without this marker, mixing intervals, for instance, with floating-point numbers produces a result flagged as NG (Not Guaranteed). This will allow f and Df to work properly for floating-point and interval inputs.*
2. *The functions `zero` and `one` return, respectively, the additive and multiplicative identities in the type of their argument. This ensures that f and Df to operate correctly for both floating-point and interval inputs.*

We make use of the `RadiiPolynomial` and `LinearAlgebra` libraries:

```
julia> using RadiiPolynomial, LinearAlgebra
```

Note that the `RadiiPolynomial` library automatically loads the `IntervalArithmetic` library [2], making interval arithmetic immediately available. We can now enclose rigorously the parameters a, b using interval arithmetic:

```
julia> parameters = (interval(3)/interval(4), interval(9)/interval(20)) # (a, b)
([0.75, 0.75], [0.45, 0.45])
```

2.1 Computation of the equilibria

The first task consists in identifying two distinct equilibria $c_0^*, c_1^* \in \mathbb{R}^3$ such that $f(c_0^*) = f(c_1^*) = 0$. By inspection, $c_0^* = (0, 0, 0)$ is an equilibrium of (4). For the non-trivial equilibrium c_1^* , the vector field (4) is simple enough that an explicit formula could be obtained by hand; however, we use its validation as an easy first application of the `RadiiPolynomial` Theorem 1.1.

The *equilibrium problem* involves the vector field f , its Jacobian Df and the parameters a, b . We begin by creating a data structure `EquilibriumProblem` bundling together these elements.

```
struct EquilibriumProblem
  f
  Df
  parameters
end
```

```
julia> pb = EquilibriumProblem(f, Df, parameters)
EquilibriumProblem(f, Df, ([0.75, 0.75], [0.45, 0.45]))
```

The next four paragraphs provide the steps to apply and implement the Radii Polynomial Theorem 1.1.

Step 1: Defining the zero-finding problem. An equilibrium is a zero of the vector field $f : \mathbb{R}^3 \rightarrow \mathbb{R}^3$, where we choose to endow \mathbb{R}^3 with the 1-norm

$$\|c\|_{\mathbb{R}^3} \stackrel{\text{def}}{=} \sum_{i=1}^3 |c^{(i)}|, \quad \text{for all } c = (c^{(1)}, c^{(2)}, c^{(3)}) \in \mathbb{R}^3. \quad (5)$$

Hence, we apply the Radii Polynomial Theorem 1.1 with $F = f$ on $X = \mathbb{R}^3$. The implementation is therefore straightforward.

```
F(pb::EquilibriumProblem, c) = pb.f(c, pb.parameters)
```

```
DF(pb::EquilibriumProblem, c) = pb.Df(c, pb.parameters)
```

Step 2: Computing the approximate zero (with floating-point arithmetic). We compute an accurate approximation $\bar{c} \in \mathbb{R}^3$ of the equilibrium using Newton's method, which is executed via the `newton` function available from the software library `RadiiPolynomial`. Importantly, interval arithmetic is not needed at this stage; we replace the interval parameters in `EquilibriumProblem` by their midpoints.

```
function approximate_zero(pb_approx::EquilibriumProblem, c_init)
    F_DF(c) = F(pb_approx, c), DF(pb_approx, c)
    c_bar, newton_success = newton(F_DF, c_init)
    return c_bar, newton_success
end
```

```
julia> pb_approx = EquilibriumProblem(pb.f, pb.Df, mid.(pb.parameters))
EquilibriumProblem(f, Df, (0.75, 0.44999999999999996))

julia> c1_bar, newton_success = approximate_zero(pb_approx, [1.0, 0.0, 1.0])
([0.6708203932499369, 0.0, 1.0], true)
```

Step 3: Constructing the approximate inverse (with floating-point arithmetic). The construction of A is straightforward in finite dimensions. Indeed, $DF(\bar{c}) = Df(\bar{c})$ is a matrix and we can rely on a numerical algorithm to produce an approximate inverse matrix. We therefore compute $A \approx DF(\bar{c})^{-1}$ numerically using Julia's built-in `inv` function.

```
function approximate_inverse(pb_approx::EquilibriumProblem, c_bar)
    return inv(DF(pb_approx, c_bar))
end
```

```
julia> A = approximate_inverse(pb_approx, c1_bar)
3×3 Matrix{Float64}:
-0.375  -0.5  0.745356
 1.0    0.0  0.0
-1.11803 -1.49071 0.0
```

Step 4: Estimating the bounds (with interval arithmetic). The Y bound

$$Y = \|AF(\bar{c})\|_{\mathbb{R}^3} \quad (6)$$

consists of taking the 1-norm of a matrix-vector product, which is accomplished directly using interval arithmetic.

For a fixed $R \geq 0$, the calculation of $Z = Z(R)$ requires taking a supremum over the closed ball $B(\bar{c}, R)$. As $B(\bar{c}, R)$ sits in the finite-dimensional space $X = \mathbb{R}^3$ endowed with the 1-norm topology, we can enclose it by a three-dimensional *interval box*:

$$B(\bar{c}, R) \subset \text{Box}(\bar{c}, R) = \begin{pmatrix} [\bar{c}^{(1)} - R, \bar{c}^{(1)} + R] \\ [\bar{c}^{(2)} - R, \bar{c}^{(2)} + R] \\ [\bar{c}^{(3)} - R, \bar{c}^{(3)} + R] \end{pmatrix}. \quad (7)$$

We make the heuristic choice that $R \sim 10Y$, and compute

$$Z = \|I - ADf(\text{Box}(\bar{c}, R))\|_{\mathcal{B}(\mathbb{R}^3)}. \quad (8)$$

Once Y and Z have been computed, we can check the contraction criterion $Z < 1$. Upon its verification, the computer-assisted proof has succeeded, and the Radii Polynomial Theorem 1.1 yields an *interval of existence* whose infimum $r = Y/(1 - Z)$, is a rigorous a posteriori error bound, with respect to the norm $\|\cdot\|_{\mathbb{R}^3}$, on the approximate equilibrium \bar{c} . This verification is done using the `interval_of_existence` function provided by the `RadiiPolynomial` library, which returns the interval of existence together with a Boolean value `true`, or `false`, signaling the success, or failure, of the computer-assisted proof.

```
Y_bound(pb::EquilibriumProblem, c_bar, A) = norm(A * F(pb, c_bar), 1)
```

```
function Z_bound(pb::EquilibriumProblem, c_bar, A, R)
    box_c = interval.(c_bar, R; format = :midpoint)
    return opnorm(interval(I) - A * DF(pb, box_c), 1)
end
```

```
julia> Y = Y_bound(pb, interval(c1_bar), interval(A))
[0.0, 8.27511e-17]

julia> R = interval(10sup(Y))
[8.27511e-16, 8.27511e-16]

julia> Z_bound(pb, interval(c1_bar), interval(A), R)
[6.93889e-17, 3.32242e-15]

julia> ie, proof_success = interval_of_existence(Y, Z, R)
([8.27511e-17, 8.27511e-16]_com, true)

julia> r_inf = inf(ie)
8.275113844157605e-17

julia> c1_star = interval.(c1_bar, r_inf; format = :midpoint)
3-element Vector{Interval{Float64}}:
 [0.67082, 0.67082]
 [-8.27511e-17, 8.27511e-17]
 [1.0, 1.0]
```

In the above last line of code evaluation, we represent the mathematically exact equilibrium

c^* , proven to lie in $B(\bar{c}, r)$, as the interval box

$$c^* \in \text{Box}(\bar{c}, r) = \begin{pmatrix} [\bar{c}^{(1)} - r, \bar{c}^{(1)} + r] \\ [\bar{c}^{(2)} - r, \bar{c}^{(2)} + r] \\ [\bar{c}^{(3)} - r, \bar{c}^{(3)} + r] \end{pmatrix}. \quad (9)$$

2.2 Computation of the eigenspaces

Having determined the two equilibria $c_0^*, c_1^* \in \mathbb{R}^3$, we now recover the stable and unstable eigenspaces. To achieve this, for each $i = 0, 1$, we solve the eigenvalue problem

$$Df(c_i^*)v = \lambda v. \quad (10)$$

Provided that the eigenvalues are simple, an adequate zero-finding problem is

$$\begin{pmatrix} Df(c_i^*)v - \lambda v \\ v^{(l_*)} - 1 \end{pmatrix} = 0, \quad (v, \lambda) \in \mathbb{C}^3 \times \mathbb{C}, \quad (11)$$

for some fixed index $l_* \in \{1, 2, 3\}$. The equation $v^{(l_*)} - 1 = 0$ is a *normalization condition* to isolate the eigenvector in $\ker(Df(c_i^*) - \lambda I)$, which is enough when the kernel is one-dimensional.

This is again a finite-dimensional problem, and we can apply the Radii Polynomial Theorem 1.1 with $F = F_{\text{eig}}$ on $X = \mathbb{C}^3 \times \mathbb{C}$, following the same steps as we did in the proof of the equilibria. Since the procedure is virtually identical, we do not repeat it, and only summarize the obtained result:

1. c_0^* is a saddle equilibrium with *two real stable eigenvalues* and one real unstable eigenvalue.
2. c_1^* is a saddle equilibrium with one stable eigenvalue and *two complex conjugate unstable eigenvalues*.

3 Validated computation of invariant manifolds

We now turn to the nonlinear analogues of the eigenspaces, which will be used to set up the boundary-value problem proving the existence of a connecting orbit. The classical (Un)Stable Manifold Theorem guarantees the existence of a local manifold, invariant under the flow, as the image of a graph over the (un)stable eigenspace [8]. To state things briefly, denoting by $\varphi_t : \mathbb{R}^3 \rightarrow \mathbb{R}^3$ the flow associated with the Shimizu–Morioka system (1), the local stable and unstable manifolds consist of the set of initial conditions in phase space such that

$$W_{loc}^s(c) = \left\{ \phi \in \text{neighbourhood of } c : \lim_{t \rightarrow +\infty} \varphi_t(\phi) = c \right\}, \quad (12a)$$

$$W_{loc}^u(c) = \left\{ \phi \in \text{neighbourhood of } c : \lim_{t \rightarrow -\infty} \varphi_t(\phi) = c \right\}. \quad (12b)$$

Under some *mild non-resonance condition* (detailed below), it is in fact possible to parameterize the local manifold without requiring it to be a graph; this strategy is called the *parameterization method* [4, 5, 6, 1]. This parameterization P defines a diffeomorphism, mapping a portion of the eigenspace onto the local invariant manifold.

Let $c \in \mathbb{R}^3$ be an equilibrium of f , and $\lambda = (\lambda_1, \dots, \lambda_d)$ the collection of all the $d \geq 1$ stable (resp. unstable) eigenvalues of $Df(c)$. We denote by Λ the d -by- d diagonal matrix whose diagonal entries are given by λ . The Hartman–Grobman Theorem [8] states that the linear and nonlinear dynamics near a hyperbolic equilibrium are topologically conjugate. Motivated by

this, we look for $P : U \subset \mathbb{C}^d \rightarrow \mathbb{C}^3$ as a *topological conjugacy* between the (unknown) nonlinear flow φ_t and the linear flow $e^{\Lambda t}$ restricted to the stable (resp. unstable) eigenspace:

$$\varphi_t \circ P = P \circ e^{\Lambda t}, \quad P(0) = c. \quad (13)$$

Then, the infinitesimal version of the conjugacy relation (13) is obtained by differentiating with respect to t at $t = 0$:

$$DP(\theta)\Lambda\theta = f(P(\theta)). \quad (14)$$

In words, the above *invariance equation* means that $DP(\theta)$ maps the tangent vector $\Lambda\theta \in \mathbb{C}^d$ to a vector tangent to $P(U) \subset \mathbb{C}^3$. The image $P(U)$ is the immersed local stable (resp. unstable) manifold.

Remark 3.1 (Real image of the parameterization). *For two real eigenvalues, the parameterization is real-valued on the real domain, namely $P : U \cap \mathbb{R}^2 \rightarrow \mathbb{R}^3$. For a pair of complex conjugate eigenvalues, the parameterization instead satisfies the conjugation symmetry*

$$P(\theta_2^*, \theta_1^*) = P(\theta_1, \theta_2)^*, \quad (15)$$

with the superscript $*$ denoting complex conjugation. Thus, the restriction of P to $\{(\rho e^{i\alpha}, \rho e^{-i\alpha}) : (\rho, \alpha) \in \mathbb{R}^2\} \cap U$ is real-valued, and recovers the local invariant manifold.

We consider a Taylor series expansion of $P = (P^{(1)}, P^{(2)}, P^{(3)})$, i.e.,

$$P(\theta) = \sum_{k=(k_1, \dots, k_d) \in \mathbb{N}_0^d} P_k \theta^k, \quad \theta^k = \theta_1^{k_1} \dots \theta_d^{k_d}, \quad P_k = (P_k^{(1)}, P_k^{(2)}, P_k^{(3)}), \quad (16)$$

where $\mathbb{N}_0 \stackrel{\text{def}}{=} \{0, 1, 2, \dots\}$. There are two important observations which we give without proof (see, e.g., [4, 36]):

1. A necessary condition for the solvability of (14) is that the stable (resp. unstable) eigenvalues $\lambda_1, \dots, \lambda_d$ satisfy the *non-resonance condition*

$$\lambda_i = k_1 \lambda_1 + \dots + k_d \lambda_d \quad \text{if and only if} \quad k_j = \begin{cases} 1, & j = i, \\ 0, & j \neq i. \end{cases} \quad (17)$$

2. The scaling of the corresponding eigenvectors $v_1, \dots, v_d \in \mathbb{C}^3$ controls the size of the image of P and its radius of convergence.

In light of the above discussion, the *manifold problem* involves the vector field f , its Jacobian Df , the parameters a, b , as well as the rigorously validated objects from Section 2: the equilibrium c^* with the associated collection of (un)stable eigenvalues $\lambda_1^*, \dots, \lambda_d^*$ and eigenvectors v_1^*, \dots, v_d^* . We store all of these in a data structure.

```

struct ManifoldProblem
    f
    Df
    parameters
    equilibrium
    eigvals
    eigvecs
end

```

Step 1: Defining the zero-finding problem. We observed in Section 2.2 that the stable and unstable eigenspaces are two-dimensional, and so $d = 2$. Thus, we look for a bivariate Taylor series P , whose components $P^{(i)}$ belong to the space

$$X_{T,\nu}^{\otimes 2} \stackrel{\text{def}}{=} \left\{ u(\theta_1, \theta_2) = \sum_{k_1, k_2 \geq 0} u_{(k_1, k_2)} \theta_1^{k_1} \theta_2^{k_2} : \|u\|_{X_{T,\nu}^{\otimes 2}} \stackrel{\text{def}}{=} \sum_{k_1, k_2 \geq 0} |u_{(k_1, k_2)}| \nu^{k_1 + k_2} < \infty \right\}. \quad (18)$$

Note that power series in that space are analytic inside the *polydisk of radius ν*

$$\mathbb{D}_\nu^2 \stackrel{\text{def}}{=} \{(z_1, z_2) \in \mathbb{C}^2 : |z_1| < \nu, |z_2| < \nu\}. \quad (19)$$

Substituting the power series into (14), we obtain the infinite system of equations

$$\begin{aligned} \text{(zero order)} \quad & f(P_{(0,0)}) = 0, \\ \text{(first order)} \quad & Df(P_{(0,0)}) P_{(1,0)} = \lambda_1 P_{(1,0)}, \\ & Df(P_{(0,0)}) P_{(0,1)} = \lambda_2 P_{(0,1)}, \\ \text{(higher order)} \quad & (k \cdot \lambda) P_k = [f(P)]_k, \quad k_1 + k_2 \geq 2. \end{aligned} \quad (20)$$

As expected, $P_{(0,0)}$ corresponds to the equilibrium, while $P_{(1,0)}, P_{(0,1)}$ are the two stable (resp. unstable) eigenvectors. At first order, the equation simply expresses that the stable (resp. unstable) eigenspace is tangent to the stable (resp. unstable) manifold at the equilibrium.

Consider the Banach space

$$\mathcal{X}_{T,\nu} \stackrel{\text{def}}{=} \left(X_{T,\nu}^{\otimes 2} \right)^3, \quad \|P\|_{\mathcal{X}_{T,\nu}} \stackrel{\text{def}}{=} \sum_{i=1}^3 \|P^{(i)}\|_{X_{T,\nu}^{\otimes 2}}, \quad \text{for all } P = (P^{(1)}, P^{(2)}, P^{(3)}) \in \mathcal{X}_{T,\nu}. \quad (21)$$

We can then rewrite the set of equations (20) as the zero-finding problem $F : \mathcal{X}_{T,\nu} \rightarrow \mathcal{X}_{T,\nu}$ given by

$$F(P) \stackrel{\text{def}}{=} P - \phi - \text{Diag}(\mathcal{L}_T) f(P), \quad (22)$$

where, using the validated computation of the equilibrium c^* and (un)stable eigenpairs $(v_1^*, \lambda_1^*), (v_2^*, \lambda_2^*)$ from Section 2,

$$\phi(\theta) = c^* + v_1^* \theta_1 + v_2^* \theta_2, \quad (23)$$

and,

$$\text{Diag}(\mathcal{L}_T) \stackrel{\text{def}}{=} \begin{pmatrix} \mathcal{L}_T & 0 & 0 \\ 0 & \mathcal{L}_T & 0 \\ 0 & 0 & \mathcal{L}_T \end{pmatrix}, \quad (\mathcal{L}_T)_{k,l} \stackrel{\text{def}}{=} \begin{cases} (k_1 \lambda_1^* + k_2 \lambda_2^*)^{-1}, & k = l, k_1 + k_2 \geq 2, \\ 0, & \text{otherwise.} \end{cases} \quad (24)$$

In the `RadiiPolynomial` library, a `Sequence` stores the coefficients of an expansion in a prescribed basis (Taylor, Fourier, Chebyshev, ...), with the basis encoded as a type parameter; tensor products of bases are assembled via `TensorSpace`, so that `TensorSpace{NTuple{2,Taylor}}` is the space of bivariate Taylor series relevant here. Linear operators acting on such sequences likewise carry their domain and codomain in their type, and a hierarchy of abstract types (e.g., `AbstractDiagonalOperator`) groups them by structure. We therefore implement \mathcal{L}_T as a new data type `L_manifold` declared to be a subtype (via `<:`) of `AbstractDiagonalOperator`, and we specify its action by overloading the `getcoefficient` function from the `RadiiPolynomial` library: each matrix entry is indexed by a pair (codom, k) , (dom, l) of $(\text{space}, \text{multi-index})$, and, as per the definition of \mathcal{L}_T given in (24), the method returns $(k_1 \lambda_1 + k_2 \lambda_2)^{-1}$ when $k = l$ and $k_1 + k_2 \geq 2$, and zero otherwise.

```

struct L_manifold <: AbstractDiagonalOperator
    λ1
    λ2
end

function RadiiPolynomial.getcoefficient(L::L_manifold, (codom, k)::T, (dom, l)::T) where
    ↪ {T<:Tuple{TensorSpace{NTuple{2,Taylor}},NTuple{2,Int}}}
    x = inv(exact(k[1]) * L.λ1 + exact(k[2]) * L.λ2)
    k == l && sum(k) ≥ 2 && return x
    return zero(x)
end

```

Furthermore, we note that $X_{T,\nu}^{\otimes 2}$ comes naturally equipped with a multiplication operation, the *Cauchy product*, so that for any $P, Q \in X_{T,\nu}^{\otimes 2}$, we have

$$P(\theta)Q(\theta) = (P * Q)(\theta) = \sum_{k_1, k_2 \geq 0} (P * Q)_{(k_1, k_2)} \theta_1^{k_1} \theta_2^{k_2}, \quad (25)$$

$$\text{where } (P * Q)_{(k_1, k_2)} \stackrel{\text{def}}{=} \sum_{l_1=0}^{k_1} \sum_{l_2=0}^{k_2} P_{(k_1-l_1, k_2-l_2)} Q_{(l_1, l_2)}.$$

In fact, $(X_{T,\nu}^{\otimes 2}, *)$ forms a Banach algebra as $\|P * Q\|_{X_{T,\nu}^{\otimes 2}} \leq \|P\|_{X_{T,\nu}^{\otimes 2}} \|Q\|_{X_{T,\nu}^{\otimes 2}}$. Hence, the vector field $f : \mathbb{R}^3 \rightarrow \mathbb{R}^3$ naturally extends as a map acting on $\mathcal{X}_{T,\nu}$, and we use the same notation to denote this map $f : \mathcal{X}_{T,\nu} \rightarrow \mathcal{X}_{T,\nu}$, so that

$$f(P) = \begin{pmatrix} P^{(2)} \\ P^{(1)} - aP^{(2)} - P^{(1)} * P^{(3)} \\ -bP^{(3)} + P^{(1)} * P^{(1)} \end{pmatrix}, \quad \text{for all } P = (P^{(1)}, P^{(2)}, P^{(3)}) \in \mathcal{X}_{T,\nu}. \quad (26)$$

```

function F(pb::ManifoldProblem, u)
    L = L_manifold(pb.eigvals[1], pb.eigvals[2])

    θ1 = Sequence(Taylor(1) ⊗ Taylor(0), [exact(0), exact(1)])
    θ2 = Sequence(Taylor(0) ⊗ Taylor(1), [exact(0), exact(1)])
    φ = pb.equilibrium + pb.eigvecs[:,1] .* θ1 + pb.eigvecs[:,2] .* θ2

    return u - φ - L .* pb.f(u, pb.parameters)
end

function DF(pb::ManifoldProblem, u)
    L = L_manifold(pb.eigvals[1], pb.eigvals[2])

    return Diagonal([exact(I), exact(I), exact(I)]) - L .* Multiplication.(pb.Df(u,
    ↪ pb.parameters))
end

```

Step 2: Computing the approximate zero (with floating-point arithmetic). We wish to obtain a polynomial approximation of order $K \geq 2$ of the manifold

$$\bar{P}(\theta) = \sum_{k_1=0}^K \sum_{k_2=0}^K \bar{P}_{(k_1, k_2)} \theta_1^{k_1} \theta_2^{k_2}, \quad (27)$$

Formally, we introduce the projection operator $\Pi_{\leq K} : X_{T,\nu}^{\otimes 2} \rightarrow X_{T,\nu}^{\otimes 2}$ defined by

$$(\Pi_{\leq K} P)_k \stackrel{\text{def}}{=} \begin{cases} P_k, & \max(k_1, k_2) \leq K, \\ 0, & \max(k_1, k_2) > K, \end{cases} \quad k = (k_1, k_2) \in \mathbb{N}_0^2. \quad (28)$$

This approximation of $DF(\bar{P})$ is far easier to invert: letting $A_{\leq K} \approx (\Pi_{\leq K} DF(\bar{P}) \Pi_{\leq K})^{-1}$ (i.e., the inverse of a $3(K+1)^2$ -by- $3(K+1)^2$ matrix), we set

$$A = A_{\leq K} \Pi_{\leq K} + \Pi_{> K}. \quad (34)$$

```

function approximate_inverse(pb_approx::ManifoldProblem, P_bar)
    Π = Projection(space(P_bar))
    A_finite = inv(mid(Π * DF(pb_approx, block(P_bar)) * Π))
    A = interval(A_finite) + (interval(I) - interval(Π))
    return A
end

```

Remark 3.2. *That we chose $K \geq 1$ to be the same for \bar{P} and A is only for convenience and to avoid introducing too many symbols; but in principle, these may be chosen independently.*

Step 4: Estimating the bounds (with interval arithmetic). The first observation is that the Y bound consists only of a finite number of calculations and is therefore directly computable. Indeed, $\bar{P} \in \Pi_{\leq K} \mathcal{X}_{T,\nu}$, and since \mathcal{L}_T is diagonal and f is quadratic, $F(\bar{P}) \in \Pi_{\leq 2K} \mathcal{X}_{T,\nu}$. By construction, A preserves this truncation order, so $AF(\bar{P}) \in \Pi_{\leq 2K} \mathcal{X}_{T,\nu}$, and therefore

$$\|AF(\bar{P})\|_{\mathcal{X}_{T,\nu}} = \sum_{i=1}^3 \left\| \sum_{j=1}^3 \Pi_{\leq 2K} A^{(i,j)} F^{(j)}(\bar{P}) \right\|_{\mathcal{X}_{T,\nu}^{\otimes 2}}. \quad (35)$$

Since the $Z(R)$ bound in the Radii Polynomial Theorem 1.1 consists in estimating the supremum of the operator norm of $I - ADF(P)$ over the closed ball $B(\bar{P}, R) \subset \mathcal{X}_{T,\nu}$, it requires some more analysis to derive formulas that can be estimated by a computer.

Proposition 3.3 (Formula for the Z bound). Let $K \geq 2$ and $\bar{P} \in \Pi_{\leq K} \mathcal{X}_{T,\nu}$, and $\lambda_1^*, \lambda_2^* \in \mathbb{C}$ such that $\operatorname{Re}(\lambda_1^*) \operatorname{Re}(\lambda_2^*) > 0$, i.e., both eigenvalues lie in the same half-plane. Consider the map F given in (22) and A given in (34). Consider $R \in [0, \infty]$, and $Z_0, Z_1(R) \geq 0$ satisfying

$$\max\left(\|\Pi_{\leq K} - \Pi_{\leq 2K} A \Pi_{\leq 2K} DF(\bar{P}) \Pi_{\leq K}\|_{\mathcal{B}(\mathcal{X}_{T,\nu})}, \|\Pi_{> K} \mathcal{L}_T \Pi_{> K}\|_{\mathcal{B}(\mathcal{X}_{T,\nu})} \|Df(\bar{P})\|_{\mathcal{B}(\mathcal{X}_{T,\nu})} \right) \leq Z_0, \quad (36a)$$

$$2R \|A \operatorname{Diag}(\mathcal{L}_T)\|_{\mathcal{B}(\mathcal{X}_{T,\nu})} \leq Z_1(R), \quad (36b)$$

where

$$\|\Pi_{> K} \mathcal{L}_T \Pi_{> K}\|_{\mathcal{B}(\mathcal{X}_{T,\nu})} \leq \frac{1}{(K+1) \min_{i=1,2} |\operatorname{Re}(\lambda_i^*)|}, \quad (37a)$$

$$\|A \operatorname{Diag}(\mathcal{L}_T)\|_{\mathcal{B}(\mathcal{X}_{T,\nu})} \leq \max\left(\|A_{\leq K} \operatorname{Diag}(\mathcal{L}_T) \Pi_{\leq K}\|_{\mathcal{B}(\mathcal{X}_{T,\nu})}, \|\Pi_{> K} \mathcal{L}_T \Pi_{> K}\|_{\mathcal{B}(\mathcal{X}_{T,\nu})} \right). \quad (37b)$$

Then,

$$\sup_{P \in B(\bar{P}, R)} \|I - ADF(P)\|_{\mathcal{B}(\mathcal{X}_{T,\nu})} \leq Z(R) = Z_0 + Z_1(R). \quad (38)$$

Proof. Let $P \in B(\bar{P}, R)$. The triangle inequality yields

$$\|I - ADF(P)\|_{\mathcal{B}(\mathcal{X}_{T,\nu})} \leq \|I - ADF(\bar{P})\|_{\mathcal{B}(\mathcal{X}_{T,\nu})} + \|A(DF(P) - DF(\bar{P}))\|_{\mathcal{B}(\mathcal{X}_{T,\nu})}.$$

The goal is to show that the two terms are bounded by Z_0 and $Z_1(R)$, respectively. The argument relies on two ingredients. First, since $\operatorname{Re}(\lambda_1^*) \operatorname{Re}(\lambda_2^*) > 0$, we have $|k_1 \lambda_1^* + k_2 \lambda_2^*| \geq$

$(k_1 + k_2) \min_{i=1,2} |\operatorname{Re}(\lambda_i^*)|$, so the tail bound of \mathcal{L}_T satisfies

$$\|\Pi_{>K} \mathcal{L}_T \Pi_{>K}\|_{\mathcal{B}(X_{T,\nu}^{\otimes 2})} = \sup_{\max(k_1, k_2) > K} \frac{1}{|k_1 \lambda_1^* + k_2 \lambda_2^*|} \leq \frac{1}{(K+1) \min_{i=1,2} |\operatorname{Re}(\lambda_i^*)|}.$$

Second, the operator norm on $\mathcal{X}_{T,\nu}$ decomposes as

$$\|L\|_{\mathcal{B}(\mathcal{X}_{T,\nu})} = \max \left(\|L \Pi_{\leq K}\|_{\mathcal{B}(\mathcal{X}_{T,\nu})}, \|L \Pi_{> K}\|_{\mathcal{B}(\mathcal{X}_{T,\nu})} \right), \quad \text{for all } L \in \mathcal{B}(\mathcal{X}_{T,\nu}).$$

For the $Z_1(R)$ bound, since $DF(P) - DF(\bar{P}) = -\operatorname{Diag}(\mathcal{L}_T)(Df(P) - Df(\bar{P}))$ and the only entries of

$$Df(P) = \begin{pmatrix} 0 & 1 & 0 \\ 1 - P^{(3)} & -a & -P^{(1)} \\ 2P^{(1)} & 0 & -b \end{pmatrix}$$

that depend on P are at positions $(2, 1)$, $(2, 3)$, and $(3, 1)$. A direct estimate yields

$$\|Df(P) - Df(\bar{P})\|_{\mathcal{B}(\mathcal{X}_{T,\nu})} \leq 2R.$$

Applying the operator norm decomposition above with $L = A \operatorname{Diag}(\mathcal{L}_T)$ and using $A \Pi_{>K} = \Pi_{>K}$ together with the tail bound,

$$\|A \operatorname{Diag}(\mathcal{L}_T)\|_{\mathcal{B}(\mathcal{X}_{T,\nu})} \leq \max \left(\|A_{\leq K} \operatorname{Diag}(\mathcal{L}_T) \Pi_{\leq K}\|_{\mathcal{B}(\mathcal{X}_{T,\nu})}, \frac{1}{(K+1) \min_{i=1,2} |\operatorname{Re}(\lambda_i^*)|} \right).$$

Hence, $\|A(DF(P) - DF(\bar{P}))\|_{\mathcal{B}(\mathcal{X}_{T,\nu})} \leq 2R \|A \operatorname{Diag}(\mathcal{L}_T)\|_{\mathcal{B}(\mathcal{X}_{T,\nu})} \leq Z_1(R)$ as desired.

For the Z_0 bound, applying the operator norm decomposition above with $L = I - ADF(\bar{P})$ reduces the problem to estimating $[I - ADF(\bar{P})] \Pi_{\leq K}$ and $[I - ADF(\bar{P})] \Pi_{> K}$ separately. Using $A \Pi_{>K} = \Pi_{>K}$, that \mathcal{L}_T is diagonal, and that $Df(\bar{P}) \Pi_{>K} = \Pi_{>K} Df(\bar{P}) \Pi_{>K}$ (from the property of the Cauchy product, which yields lower triangular multiplication operators), we obtain

$$[I - ADF(\bar{P})] \Pi_{>K} = \Pi_{>K} \operatorname{Diag}(\mathcal{L}_T) \Pi_{>K} Df(\bar{P}) \Pi_{>K},$$

whose norm is at most $\frac{1}{(K+1) \min_{i=1,2} |\operatorname{Re}(\lambda_i^*)|} \|Df(\bar{P})\|_{\mathcal{B}(\mathcal{X}_{T,\nu})}$ by submultiplicativity and the tail bound of \mathcal{L}_T established above. On the truncated part, since $\bar{P} \in \Pi_{\leq K} \mathcal{X}_{T,\nu}$ and f is quadratic, $DF(\bar{P}) \Pi_{\leq K} = \Pi_{\leq 2K} DF(\bar{P}) \Pi_{\leq K}$. Hence, $ADF(\bar{P}) \Pi_{\leq K} = \Pi_{\leq 2K} A \Pi_{\leq 2K} DF(\bar{P}) \Pi_{\leq K}$ is a finite matrix, and

$$\|[I - ADF(\bar{P})] \Pi_{\leq K}\|_{\mathcal{B}(\mathcal{X}_{T,\nu})} = \|\Pi_{\leq K} - \Pi_{\leq 2K} A \Pi_{\leq 2K} DF(\bar{P}) \Pi_{\leq K}\|_{\mathcal{B}(\mathcal{X}_{T,\nu})}.$$

Combining these shows that $\|I - ADF(\bar{P})\|_{\mathcal{B}(\mathcal{X}_{T,\nu})} \leq Z_0$. \square

We stress that, by construction of A , its surjectivity is equivalent to its injectivity; hence, verifying $Z(R) = Z_0 + Z_1(R) < 1$ is enough to imply that A is injective. Then, the Radii Polynomial Theorem 1.1 yields a rigorous a posteriori error bound $r = Y/(1 - Z)$, with respect to the norm $\|\cdot\|_{\mathcal{X}_{T,\nu}}$, on the polynomial approximation \bar{P} of the parameterization of the local invariant manifold. In particular, the mathematically exact parameterization P^* can be written as

$$P^* = \bar{P} + h, \quad \|h\|_{\mathcal{X}_{T,\nu}} \leq \frac{Y}{1 - Z}. \quad (39)$$

`Y_bound(pb::ManifoldProblem, P_bar, A, X) = norm(A * F(pb, block(P_bar)), X)`

`function Z_bound(pb::ManifoldProblem, P_bar, A, R, X_T, X)`
`K = order(block(P_bar, 1))[1]`

```

Π = interval(Projection(space(P_bar)))

L = Diagonal([L_manifold(pb.eigvals[1], pb.eigvals[2]) for j ∈ 1:3])
tail_bound_L = inv(interval(K + 1) * minimum(abs ∘ real, pb.eigvals))
opnorm_AL = max(opnorm(A * (L * Π), X), tail_bound_L)

B = DF(pb, block(P_bar))
W = pb.Df(block(P_bar), pb.parameters)
Z_0 = max(opnorm(Π - A * (B * Π), X),
          tail_bound_L * opnorm(norm.(W, X_T), 1))

Z_1 = exact(2) * R * opnorm_AL

return Z_0 + Z_1
end

```

4 Validated computation of transverse intersection

To not overburden the article, we do not provide the code alongside the mathematical discussion; the code, however, is available in full at [14].

We now have all the necessary pieces to prove the existence of a heteroclinic orbit connecting the two equilibria c_0^* , c_1^* , that is, we seek a solution a solution to the system (1) satisfying

$$\lim_{t \rightarrow -\infty} w(t) = c_1^*, \quad \lim_{t \rightarrow +\infty} w(t) = c_0^*. \quad (40)$$

By restricting to a finite time interval $[0, \tau]$, this can be reformulated as the boundary value problem

$$\begin{cases} \frac{d}{dt} w(t) = f(w(t)), & t \in [0, \tau], \\ w(0) \in W_{\text{loc}}^u(c_1^*), \\ w(\tau) \in W_{\text{loc}}^s(c_0^*). \end{cases} \quad (41)$$

In the previous section, rigorous parameterizations of the local invariant manifolds have been computed

$$P^* : \mathbb{D}_\nu^2 \rightarrow \mathbb{C}^3, \quad Q^* : \mathbb{D}_\nu^2 \cap \mathbb{R}^2 \rightarrow \mathbb{R}^3, \quad (42)$$

representing the unstable manifold of c_1^* and the stable manifold of c_0^* , respectively. The boundary conditions can then be written as

$$w(0) = P^*(\sigma), \quad w(\tau) = Q^*(\theta), \quad (43)$$

where $\sigma, \theta \in \mathbb{D}_\nu^2$ are local manifold coordinates.

Step 1: Defining the zero-finding problem. Beyond the trajectory $t \mapsto w(t)$, the unknowns are the local coordinates $\sigma \in \mathbb{D}_\nu^2$ on the unstable side and $\theta \in \mathbb{D}_\nu^2 \cap \mathbb{R}^2$ on the stable side, together with the integration time $\tau > 0$, totaling 5 scalar parameters. The boundary condition $w(\tau) = Q^*(\theta)$ contributes 3 scalar equations, leaving 2 degrees of freedom to fix. We do so by prescribing $\tau > 0$ and restricting the unstable coordinates to the unit circle,

$$\sigma = \gamma(\alpha) \stackrel{\text{def}}{=} (e^{i\alpha}, e^{-i\alpha}), \quad \alpha \in \mathbb{R}. \quad (44)$$

Since $\nu > 1$ was used in Section 3, we do have that $\gamma(\alpha)$ lies inside the domain of analyticity \mathbb{D}_ν^2 of the parameterization P^* of the local unstable manifold of c_1^* .

To represent the trajectory $t \mapsto w(t)$, we expand it in Chebyshev polynomials of the first kind, $T_k(s) \stackrel{\text{def}}{=} \cos(k \arccos s)$, $s \in [-1, 1]$. Unlike Taylor series, Chebyshev expansions are well-suited to non-local trajectories. In particular, an analytic function on $[-1, 1]$ admits a Chebyshev series whose coefficients decay exponentially fast. Hence, consider the Banach space, for $\mu \geq 1$,

$$X_{C,\mu} \stackrel{\text{def}}{=} \left\{ u(s) = u_0 + 2 \sum_{k \geq 1} u_k T_k(s) : \|u\|_{X_{C,\mu}} \stackrel{\text{def}}{=} |u_0| + 2 \sum_{k \geq 1} |u_k| \mu^k < \infty \right\}. \quad (45)$$

For $\mu > 1$, series in $X_{C,\mu}$ extend analytically inside the Bernstein ellipse

$$\mathbb{E}_\mu \stackrel{\text{def}}{=} \left\{ z \in \mathbb{C} : z = \frac{1}{2}(w + w^{-1}), |w| < \mu \right\}. \quad (46)$$

We refer to [33] for a thorough exposition.

We consider the time rescaling $s \in [-1, 1] \mapsto t(s) = \tau(s + 1)/2$, and introduce the rescaled trajectory $u(s) = w(t(s))$. Using the boundary conditions (43) and integrating (41) from -1 to s , we obtain

$$\begin{cases} u(s) = P^*(\gamma(\alpha)) + \frac{\tau}{2} \int_{-1}^s f(u(s')) ds', & s \in [-1, 1], \\ u(1) = Q^*(\theta). \end{cases} \quad (47)$$

Let

$$\mathcal{X}_{C,\mu} \stackrel{\text{def}}{=} X_{C,\mu}^3 \times \mathbb{R}^3, \quad \|x\|_{\mathcal{X}_{C,\mu}} \stackrel{\text{def}}{=} \sum_{i=1}^3 \|u^{(i)}\|_{X_{C,\mu}} + |\alpha| + |\theta_1| + |\theta_2|, \quad (48)$$

for all $x = (u, \alpha, \theta_1, \theta_2) \in \mathcal{X}_{C,\mu}$ with $u = (u^{(1)}, u^{(2)}, u^{(3)}) \in X_{C,\mu}^3$ and $\alpha, \theta_1, \theta_2 \in \mathbb{R}$. Then, a heteroclinic orbit can be seen as a zero of the map $F : \mathcal{X}_{C,\mu} \rightarrow \mathcal{X}_{C,\mu}$ given by

$$F(u, \alpha, \theta_1, \theta_2) \stackrel{\text{def}}{=} \begin{pmatrix} u - P^*(\gamma(\alpha)) - \frac{\tau}{2} \text{Diag}(\mathcal{L}_C) f(u) \\ u(1) - Q^*(\theta_1, \theta_2) \end{pmatrix}, \quad (49)$$

where

$$\text{Diag}(\mathcal{L}_C) \stackrel{\text{def}}{=} \begin{pmatrix} \mathcal{L}_C & 0 & 0 \\ 0 & \mathcal{L}_C & 0 \\ 0 & 0 & \mathcal{L}_C \end{pmatrix}, \quad (\mathcal{L}_C u)_k \stackrel{\text{def}}{=} \begin{cases} u_0 - \frac{u_1}{2} + 2 \sum_{l \geq 2} \frac{(-1)^{l+1}}{l^2 - 1} u_l, & k = 0, \\ \frac{u_{k-1} - u_{k+1}}{2k}, & k \geq 1. \end{cases} \quad (50)$$

As with Taylor series (see Section 3), we note that $X_{C,\mu}$ comes naturally equipped with a multiplication operation, the *discrete convolution*, so that for any $u, w \in X_{C,\mu}$, we have

$$\begin{aligned} u(s)w(s) &= (u * w)(s) = (u * w)_0 + 2 \sum_{k \geq 0} (u * w)_k T_k(s), \\ \text{where } (u * w)_k &\stackrel{\text{def}}{=} \sum_{l \in \mathbb{Z}} u_{|k-l|} w_{|l|}, \quad k \geq 0. \end{aligned} \quad (51)$$

In addition, $(X_{C,\mu}, *)$ is a Banach algebra such that $\|u * w\|_{X_{C,\mu}} \leq \|u\|_{X_{C,\mu}} \|w\|_{X_{C,\mu}}$. Once more, the vector field $f : \mathbb{R}^3 \rightarrow \mathbb{R}^3$ can be extended as a map $f : X_{C,\mu}^3 \rightarrow X_{C,\mu}^3$, where the arithmetic operations (addition and multiplication) should be understood as those of $X_{C,\mu}$.

Remark 4.1 (Notation). *We purposely use the same notation $*$ for the Cauchy product and the discrete convolution, as well as for the vector field as a map on \mathbb{R}^3 , $\mathcal{X}_{T,\nu}$ and $\mathcal{X}_{C,\mu}^3$. The reason is that they all have the same meaning (similarly to how $+$ denotes the additions of real numbers and that of vectors); moreover, they are unambiguously interpreted from the context of the operand.*

Remark 4.2 (Transversality). *We stress that the transversality of the intersection is a consequence of verifying the contraction in the Radii Polynomial Theorem 1.1. This fact relates to the local uniqueness and invertibility of DF at the zero x^* of F ; see, e.g., [17].*

To use the map F and its Fréchet derivative DF , we need to know how to rigorously evaluate the parameterizations $P^*, Q^* \in X_{T,\nu}^{\otimes 2}$ and their derivatives.

Lemma 4.3 (Formula for rigorous evaluation). Let $\nu > 1$, $P^* \in X_{T,\nu}^{\otimes 2}$, $\bar{P} \in \Pi_{\leq K} X_{T,\nu}^{\otimes 2}$ such that $\|P^* - \bar{P}\|_{X_{T,\nu}^{\otimes 2}} \leq r$. For $\theta = (\theta_1, \theta_2) \in \mathbb{D}_1^2$, it holds that

$$|P^*(\theta_1, \theta_2) - \bar{P}(\theta_1, \theta_2)| \leq r, \quad (52a)$$

$$|\partial_{\theta_j} P^*(\theta_1, \theta_2) - \partial_{\theta_j} \bar{P}(\theta_1, \theta_2)| \leq \frac{r}{e^{|\theta_j|} |\ln(|\theta_j|/\nu)|}, \quad j = 1, 2. \quad (52b)$$

Proof. The first inequality follows from $X_{T,\nu}^{\otimes 2} \subset X_{T,1}^{\otimes 2}$ together with the fact that the $X_{T,1}^{\otimes 2}$ -norm controls the supremum norm on the polydisk \mathbb{D}_1^2 . For the second inequality, denoting $h = P^* - \bar{P}$,

$$|\partial_{\theta_1} h(\theta_1, \theta_2)| \leq \sum_{k_1 \geq 1, k_2 \geq 0} k_1 |h_{(k_1, k_2)}| |\theta_1|^{k_1-1} |\theta_2|^{k_2} \leq r \sup_{k_1 \geq 1} k_1 |\theta_1|^{k_1-1} \nu^{-k_1}.$$

Let $\delta = |\theta_1| \leq 1$, the continuous extension $g(s) \stackrel{\text{def}}{=} s\delta^{-1}(\delta/\nu)^s$ has $g'(s) = \delta^{-1}(\delta/\nu)^s(1 + s \ln(\delta/\nu))$, which vanishes at $s_{\text{crit}} = -1/\ln(\delta/\nu) > 0$. Hence $\sup_{k_1 \geq 1} g(k_1) \leq g(s_{\text{crit}}) = (e\delta |\ln(\delta/\nu)|)^{-1}$. \square

In other words, the two inequalities in (52) indicate that the evaluation of P^* (similarly for Q^*) at a point (θ_1, θ_2) in the interior of the unit polydisk can be enclosed rigorously by means of interval arithmetic; i.e.,

$$P^*(\theta_1, \theta_2) \in [\bar{P}(\theta_1, \theta_2) - r, \bar{P}(\theta_1, \theta_2) + r], \quad (53a)$$

$$\partial_{\theta_j} P^*(\theta_1, \theta_2) \in \left[\partial_{\theta_j} \bar{P}(\theta_1, \theta_2) - \frac{r}{e^{|\theta_j|} |\ln(|\theta_j|/\nu)|}, \partial_{\theta_j} \bar{P}(\theta_1, \theta_2) + \frac{r}{e^{|\theta_j|} |\ln(|\theta_j|/\nu)|} \right]. \quad (53b)$$

Step 2: Computing the approximate zero (with floating-point arithmetic). We seek an approximation $\bar{x} = (\bar{u}, \bar{\alpha}, \bar{\theta}_1, \bar{\theta}_2) \in \mathcal{X}_{C,\mu}$, with

$$\bar{u}^{(i)}(s) = \bar{u}_0^{(i)} + 2 \sum_{k=1}^K \bar{u}_k^{(i)} T_k(s), \quad i = 1, 2, 3. \quad (54)$$

The solution is produced via Newton's method on the finite approximation $\Pi_{\leq K} \circ F \circ \Pi_{\leq K}$ of (49), where P^* and Q^* are replaced by their finite-dimensional approximations \bar{P} and \bar{Q} . A good initial guess is less obvious here than in the previous sections. We obtain one by integrating the ODE numerically with the `DifferentialEquations` library [26], then fitting the resulting trajectory by its Chebyshev interpolation polynomial.

Step 3: Constructing the approximate inverse (with floating-point arithmetic). The Fréchet derivative of the map F given in (49) reads

$$DF(\bar{x}) = \begin{pmatrix} \boxed{I - \frac{\tau}{2} \text{Diag}(\mathcal{L}_C) Df(\bar{u})} & -DP^*(\gamma(\bar{\alpha})) \gamma'(\bar{\alpha}) & 0 & 0 \\ \mathcal{E}_1 & 0 & -\partial_{\theta_1} Q^{*,(1)}(\bar{\theta}) & -\partial_{\theta_2} Q^{*,(1)}(\bar{\theta}) \\ \mathcal{E}_2 & 0 & -\partial_{\theta_1} Q^{*,(2)}(\bar{\theta}) & -\partial_{\theta_2} Q^{*,(2)}(\bar{\theta}) \\ \mathcal{E}_3 & 0 & -\partial_{\theta_1} Q^{*,(3)}(\bar{\theta}) & -\partial_{\theta_2} Q^{*,(3)}(\bar{\theta}) \end{pmatrix}, \quad (55)$$

where $\mathcal{E}_i : X_{C,\mu}^3 \rightarrow \mathbb{R}$ denotes the evaluation $u \mapsto u^{(i)}(1) = \mathcal{E}u^{(i)}$, with the underlying functional \mathcal{E} given by the infinite row

$$\mathcal{E} = (1 \quad 2 \quad 2 \quad 2 \quad \cdots). \quad (56)$$

We argue once more that $DF(\bar{x})$ can be approximated as a finite-dimensional perturbation of the identity. The boxed block and functionals \mathcal{E}_j are the only ones acting on the infinite-dimensional space $X_{C,\mu}^3$; the remaining entries are already finite-dimensional.

The functionals \mathcal{E}_j are easily bounded on the tail part. For $\mu > 1$,

$$\|\mathcal{E}\Pi_{>K}\|_{\mathcal{B}(X_{C,\mu},\mathbb{R})} = \sup_{l>K} \frac{|\mathcal{E}_l|}{2\mu^l} = \frac{1}{\mu^{K+1}}, \quad (57)$$

which is negligible for K large.

The boxed block is slightly more delicate. Schematically, \mathcal{L}_C has the matrix structure

$$\mathcal{L}_C \sim \begin{pmatrix} * & * & * & * & * & \cdots \\ \frac{1}{2} & 0 & -\frac{1}{2} & & & \\ & \frac{1}{4} & 0 & -\frac{1}{4} & & \\ & & \frac{1}{6} & 0 & -\frac{1}{6} & \\ & & & \ddots & \ddots & \ddots \end{pmatrix},$$

where rows $k \geq 1$ are bidiagonal with $1/(2k)$ scaling and the dense first row has rapidly decaying entries. Hence \mathcal{L}_C is compact, and its tail $\Pi_{>K}\mathcal{L}_C$ and $\mathcal{L}_C\Pi_{>K}$ have small operator norm for large K (an explicit bound is given in Proposition 4.4 below). The same logic as in Section 3 therefore applies, and for sufficiently large K ,

$$I - \frac{\tau}{2}\text{Diag}(\mathcal{L}_C)Df(\bar{u}) \approx I - \Pi_{\leq K} \left(\frac{\tau}{2}\text{Diag}(\mathcal{L}_C)Df(\bar{u}) \right) \Pi_{\leq K}.$$

We set

$$A = A_{\leq K}\Pi_{\leq K} + \Pi_{>K}, \quad A_{\leq K} \approx (\Pi_{\leq K}DF(\bar{x})\Pi_{\leq K})^{-1}. \quad (58)$$

Step 4: Estimating the bounds (with interval arithmetic). As before, the Y bound consists of a finite calculation. We conclude this section with the formula for the Z bound.

Proposition 4.4 (Formula for the Z bound). Let $K \geq 2$ and $\bar{x} = (\bar{u}, \bar{\alpha}, \bar{\theta}) \in \Pi_{\leq K}\mathcal{X}_{C,\mu}$. Consider F given in (49) and A given in (58). Consider $R \in [0, \infty]$, and $Z_0, Z_1(R) \geq 0$ satisfy

$$\max\left(\|\Pi_{\leq 2K+1} - \Pi_{\leq 3K+2}A\Pi_{\leq 3K+2}DF(\bar{x})\Pi_{\leq 2K+1}\|_{\mathcal{B}(\mathcal{X}_{C,\mu})}, \right. \\ \left. M \frac{|\tau|}{2} \|Df(\bar{u})\|_{\mathcal{B}(X_{C,\mu}^3)} \right) \leq Z_0, \quad (59a)$$

$$2R \frac{|\tau|}{2} \|A\|_{\mathcal{B}(\mathcal{X}_{C,\mu})} \|\mathcal{L}_C\|_{\mathcal{B}(X_{C,\mu})} \leq Z_1(R), \quad (59b)$$

where

$$M = \|A\Pi_{\leq 0}\|_{\mathcal{B}(\mathcal{X}_{C,\mu})} \|\Pi_{\leq 0}\mathcal{L}_C\Pi_{>K+1}\|_{\mathcal{B}(X_{C,\mu})} + \|\Pi_{>K}\mathcal{L}_C\Pi_{>K+1}\|_{\mathcal{B}(X_{C,\mu})}, \quad (60)$$

and

$$\|A\|_{\mathcal{B}(\mathcal{X}_{C,\mu})} = \max\left(\|A_{\leq K}\|_{\mathcal{B}(\mathcal{X}_{C,\mu})}, 1\right), \quad (61a)$$

$$\|\mathcal{L}_C\|_{\mathcal{B}(\mathcal{X}_{C,\mu})} = 1 + \mu, \quad (61b)$$

$$\|\Pi_{\leq 0}\mathcal{L}_C\Pi_{>K+1}\|_{\mathcal{B}(\mathcal{X}_{C,\mu})} = \frac{\mu^{-(K+2)}}{(K+2)^2 - 1}, \quad (61c)$$

$$\|\Pi_{>K}\mathcal{L}_C\Pi_{>K+1}\|_{\mathcal{B}(\mathcal{X}_{C,\mu})} = \frac{\mu^{-1}}{2(K+1)} + \frac{\mu}{2(K+3)}. \quad (61d)$$

Then,

$$\sup_{x \in B(\bar{x}, R)} \|I - ADF(x)\|_{\mathcal{B}(\mathcal{X}_{C,\mu})} \leq Z(R) = Z_0 + Z_1(R). \quad (62)$$

Proof. The bounds in (61) follow from the definitions of the operators. For $x \in B(\bar{x}, R)$, the triangle inequality yields

$$\|I - ADF(x)\|_{\mathcal{B}(\mathcal{X}_{C,\mu})} \leq \|I - ADF(\bar{x})\|_{\mathcal{B}(\mathcal{X}_{C,\mu})} + \|A(DF(x) - DF(\bar{x}))\|_{\mathcal{B}(\mathcal{X}_{C,\mu})},$$

and the second term is bounded by $Z_1(R)$ following the same reasoning as in the proof of Proposition 3.3. For the first term, since the discrete convolution product (51) makes $Df(\bar{u})$ a 3-by-3 block operator whose entries are banded operators with bandwidth K , we apply the operator norm decomposition at order $2K+1$:

$$\begin{aligned} \|I - ADF(\bar{x})\|_{\mathcal{B}(\mathcal{X}_{C,\mu})} &= \\ &= \max\left(\|[I - ADF(\bar{x})]\Pi_{\leq 2K+1}\|_{\mathcal{B}(\mathcal{X}_{C,\mu})}, \|[I - ADF(\bar{x})]\Pi_{>2K+1}\|_{\mathcal{B}(\mathcal{X}_{C,\mu})}\right). \end{aligned}$$

Using $A\Pi_{>2K+1} = \Pi_{>2K+1}$ together with $Df(\bar{u})\Pi_{>2K+1} = \Pi_{>K+1}Df(\bar{u})\Pi_{>2K+1}$,

$$[I - ADF(\bar{x})]\Pi_{>2K+1} = \frac{\tau}{2} A \text{Diag}(\mathcal{L}_C\Pi_{>K+1}) Df(\bar{u})\Pi_{>2K+1},$$

whose norm is at most

$$\begin{aligned} & \frac{|\tau|}{2} \|A\mathcal{L}_C\Pi_{>K+1}Df(\bar{u})\|_{\mathcal{B}(\mathcal{X}_{C,\mu}^3)} \\ & \leq \frac{|\tau|}{2} \|A\mathcal{L}_C\Pi_{>K+1}\|_{\mathcal{B}(\mathcal{X}_{C,\mu}^3)} \|Df(\bar{u})\|_{\mathcal{B}(\mathcal{X}_{C,\mu}^3)} \\ & = \frac{|\tau|}{2} \|A\Pi_{\leq 0}\mathcal{L}_C\Pi_{>K+1} + A\Pi_{>0}\mathcal{L}_C\Pi_{>K+1}\|_{\mathcal{B}(\mathcal{X}_{C,\mu}^3)} \|Df(\bar{u})\|_{\mathcal{B}(\mathcal{X}_{C,\mu}^3)} \\ & \leq \frac{|\tau|}{2} \left(\|A\Pi_{\leq 0}\mathcal{L}_C\Pi_{>K+1}\|_{\mathcal{B}(\mathcal{X}_{C,\mu}^3)} + \|\Pi_{>K}\mathcal{L}_C\Pi_{>K+1}\|_{\mathcal{B}(\mathcal{X}_{C,\mu}^3)} \right) \|Df(\bar{u})\|_{\mathcal{B}(\mathcal{X}_{C,\mu}^3)}, \end{aligned}$$

by submultiplicativity. Since $\bar{u} \in \Pi_{\leq K}\mathcal{X}_{C,\mu}$, f is quadratic and \mathcal{L}_C has a lower diagonal, $DF(\bar{x})\Pi_{\leq 2K+1} = \Pi_{\leq 3K+2}DF(\bar{x})\Pi_{\leq 2K+1}$, so the truncated part reduces to the finite matrix $\Pi_{\leq 2K+1} - \Pi_{\leq 3K+2}A\Pi_{\leq 3K+2}DF(\bar{x})\Pi_{\leq 2K+1}$. \square

5 Conclusion

We have given a computer-assisted proof of a transverse heteroclinic orbit in the Shimizu–Morioka system, following the strategy of [17]. The argument splits into the validation of the equilibria and eigenpairs (Section 2), of the local invariant manifolds (Section 3), and of the connecting orbit (Section 4). Each subproblem follows the same four-step template: a zero-finding map F , an approximate zero \bar{x} , an approximate inverse A , and bounds Y and Z . The

Radii Polynomial Theorem 1.1, in each case, closes the argument. Note that the estimates favor clarity over sharpness, but tighter and more efficient bounds would matter for problems where errors compound across the validations.

The analysis presented in this article can be readily adapted to other systems of autonomous ordinary differential equations. More broadly, the maps F in Sections 3 and 4 are built around the form $x - \phi - \mathcal{L}f(x)$, with \mathcal{L} compact. This same structure appears in other zero-finding formulations of dynamical systems problems, such as initial-value problems and periodic orbits, for which analogues of Propositions 3.3 and 4.4 can be obtained by similar arguments.

On that note, the proofs of Propositions 3.3 and 4.4 exploit the quadratic nature of the Shimizu–Morioka vector field. For higher-degree polynomial, and even non-polynomial, nonlinearities, the underlying argument still applies through the splitting

$$\|I - ADF(x)\| \leq \|I - AB\| + \|A(B - DF(x))\|,$$

where $B = DF(\bar{x})$ is replaced by $B = I - \mathcal{L}W$, with $W \approx Df(\bar{x})$ an approximation of the multiplication operator (for instance, obtained via interpolation). The Z_0 analysis is unchanged since W retains a banded structure as a (possibly, block-wise) multiplication operator. The principal new difficulty is the control of the term $\|W - Df(x)\|$, which requires knowing how to control the nonlinearities in the relevant function space.

Acknowledgement

O. Hénot was supported by the National Science and Technology Council (NSTC) under grant No. 115-2115-M-002-001-MY2. A. Takayasu was supported by the Japan Science and Technology Agency (JST) through the FOREST Program under grant No. JPMJFR246A, and JSPS KAKENHI under grant No. 24K00538 and No. 26K00619.

References

- [1] Àlex Haro, Marta Canadell, Jordi-Lluís Figueras, Alejandro Luque, and Josep Maria Mondelo. *The Parameterization Method for Invariant Manifolds: From Rigorous Results to Effective Computations*, volume 195 of *Applied Mathematical Sciences*. Springer, Cham, 2016.
- [2] Luis Benet, Olivier Hénot, Benoît Richard, and David P. Sanders. IntervalArithmetic.jl. <https://github.com/JuliaIntervals/IntervalArithmetic.jl>, 2025. Software.
- [3] Jeff Bezanson, Alan Edelman, Stefan Karpinski, and Viral B Shah. Julia: A fresh approach to numerical computing. *SIAM Rev.*, 59(1):65–98, 2017.
- [4] X. Cabré, E. Fontich, and R. de la Llave. The parameterization method for invariant manifolds. I. Manifolds associated to non-resonant subspaces. *Indiana Univ. Math. J.*, 52(2):283–328, 2003.
- [5] X. Cabré, E. Fontich, and R. de la Llave. The parameterization method for invariant manifolds. II. Regularity with respect to parameters. *Indiana Univ. Math. J.*, 52(2):329–360, 2003.
- [6] X. Cabré, E. Fontich, and R. de la Llave. The parameterization method for invariant manifolds. III. Overview and applications. *J. Differential Equations*, 218(2):444–515, 2005.
- [7] Renato Calleja, Carlos García-Azpeitia, Olivier Hénot, Jean-Philippe Lessard, and Jason D Mireles James. From the Lagrange triangle to the figure eight choreography: Proof of Marchal’s conjecture. *Transactions of the American Mathematical Society*, 2026.

- [8] Carmen Chicone. *Ordinary Differential Equations with Applications*, volume 34 of *Texts in Applied Mathematics*. Springer, Cham, 3rd edition, 2024.
- [9] Simon Danisch and Julius Krumbiegel. Makie.jl: Flexible high-performance data visualization for Julia. *Journal of Open Source Software*, 6(65):3349, 2021.
- [10] Gabriel William Duchesne, Jean-Philippe Lessard, and Akitoshi Takayasu. A rigorous integrator and global existence for higher-dimensional semilinear parabolic PDEs via semigroup theory. *Journal of Scientific Computing*, 102(2):62, 2025.
- [11] Herman H. Goldstine. *A History of Numerical Analysis from the 16th Through the 19th Century*, volume 2 of *Studies in the History of Mathematics and Physical Sciences*. Springer-Verlag, New York, 1977.
- [12] Javier Gómez-Serrano. Computer-assisted proofs in PDE: a survey. *SeMA Journal*, 76(3):459–484, 2019.
- [13] Olivier Hénot. RadiiPolynomial.jl. <https://github.com/OlivierHnt/RadiiPolynomial.jl>, 2021. Software.
- [14] Olivier Hénot and Akitoshi Takayasu. ShimizuMoriokaTutorial. <https://github.com/OlivierHnt/ShimizuMoriokaTutorial.jl>, 2026. Software.
- [15] Allan Hungria, Jean-Philippe Lessard, and Jason D. Mireles James. Rigorous numerics for analytic solutions of differential equations: the radii polynomial approach. *Mathematics of Computation*, 85(299):1427–1459, 2016.
- [16] Jonathan Jaquette. A proof of Jones’ conjecture. *Journal of Differential Equations*, 266(6):3818–3859, 2019.
- [17] Jean-Philippe Lessard, Jason D. Mireles James, and Christian Reinhardt. Computer-assisted proof of transverse saddle-to-saddle connecting orbits for first order vector fields. *Journal of Dynamics and Differential Equations*, 26(2):267–313, 2014.
- [18] Edward N. Lorenz. Deterministic nonperiodic flow. *Journal of the Atmospheric Sciences*, 20(2):130–141, 1963.
- [19] Mitsuhiro T. Nakao. A numerical approach to the proof of existence of solutions for elliptic problems. *Japan Journal of Industrial and Applied Mathematics*, 5(2):313–332, 1988.
- [20] Mitsuhiro T. Nakao, Michael Plum, and Yoshitaka Watanabe. *Numerical verification methods and computer-assisted proofs for partial differential equations*, volume 53 of *Springer Series in Computational Mathematics*. Springer, Singapore, [2019] ©2019.
- [21] Mitsuhiro T. Nakao and Yoshitaka Watanabe. *Learning Verified Numerical Computations through Examples: Theory and Implementation*. Saiensu-sha, Tokyo, 2011. in Japanese.
- [22] Mitsuhiro T. Nakao and Nobito Yamamoto. *Verified Numerical Computations — A Computational Challenge to Infinity*. Tutorial: Frontiers of Applied Mathematics. Nihon Hyoron Sha, Tokyo, 1998. in Japanese.
- [23] Shin’ichi Oishi. Numerical verification of existence and inclusion of solutions for nonlinear operator equations. *Journal of Computational and Applied Mathematics*, 60:171–185, 1995.
- [24] Shin’ichi Oishi, editor. *Principles of Verified Numerical Computations*. Corona Publishing, Tokyo, 2018. in Japanese.

- [25] Shin’ichi Oishi and Siegfried M. Rump. Fast verification of solutions of matrix equations. *Numerische Mathematik*, 90(4):755–773, 2002.
- [26] Christopher Rackauckas and Qing Nie. DifferentialEquations.jl – a performant and feature-rich ecosystem for solving differential equations in Julia. *Journal of Open Research Software*, 5(1):15, 2017.
- [27] Siegfried M. Rump. INTLAB — INTerval LABoratory. In Tibor Csendes, editor, *Developments in Reliable Computing*, pages 77–104. Kluwer Academic Publishers, Dordrecht, 1999.
- [28] Siegfried M. Rump. Verification methods: Rigorous results using floating-point arithmetic. *Acta Numerica*, 19:287–449, 2010.
- [29] Kouta Sekine, Mitsuhiro T. Nakao, and Shin’ichi Oishi. A new formulation using the Schur complement for the numerical existence proof of solutions to elliptic problems: without direct estimation for an inverse of the linearized operator. *Numerische Mathematik*, 146(4):907–926, 2020.
- [30] T. Shimizu and N. Morioka. On the bifurcation of a symmetric limit cycle to an asymmetric one in a simple model. *Physics Letters A*, 76(3):201–204, 1980.
- [31] Teruo Sunaga. Theory of an interval algebra and its application to numerical analysis. *RAAG Memoirs*, 2:29–46, 1958. Reprinted in Japan J. Ind. Appl. Math. **26** (2009), 125–143.
- [32] Akitoshi Takayasu, Jean-Philippe Lessard, Jonathan Jaquette, and Hisashi Okamoto. Rigorous numerics for nonlinear heat equations in the complex plane of time. *Numerische Mathematik*, 151(3):693–750, 2022.
- [33] Lloyd N. Trefethen. *Approximation theory and approximation practice*. Society for Industrial and Applied Mathematics (SIAM), Philadelphia, PA, 2013.
- [34] Warwick Tucker. A rigorous ODE solver and Smale’s 14th problem. *Foundations of Computational Mathematics*, 2(1):53–117, 2002.
- [35] Minoru Urabe. Galerkin’s procedure for nonlinear periodic systems. *Archive for Rational Mechanics and Analysis*, 20:120–152, 1965.
- [36] Jan Bouwe van den Berg, Jason D. Mireles James, and Christian Reinhardt. Computing (un)stable manifolds with validated error bounds: Non-resonant and resonant spectra. *Journal of Nonlinear Science*, 26(4):1055–1095, 2016.
- [37] Jan Bouwe van den Berg and Jonathan Jaquette. A proof of Wright’s conjecture. *Journal of Differential Equations*, 264(12):7412–7462, 2018.
- [38] Jan Bouwe van den Berg and Jean-Philippe Lessard, editors. *Rigorous Numerics in Dynamics*, volume 74 of *Proceedings of Symposia in Applied Mathematics*. American Mathematical Society, Providence, RI, 2018.
- [39] Nobito Yamamoto. A numerical verification method for solutions of boundary value problems with local uniqueness by Banach’s fixed-point theorem. *SIAM Journal on Numerical Analysis*, 35(5):2004–2013, 1998.